

Deterministic Molecular Assembly with a Finite Set of Building Blocks: Universal Assembly Kits for Backbone-Assisted and Sequence-Directed Abstract Tile Assembly Models

Jeremy Guntoro^{1*} and Thomas Ouldridge^{1,2*}

¹Department of Bioengineering, Imperial College London, Exhibition road, London, SW72AZ, United Kingdom.

²Imperial College Centre for Synthetic Biology, Imperial College London, Exhibition road, London, SW72AZ, United Kingdom.

*Corresponding author(s). E-mail(s): jeremy.guntoro16@imperial.ac.uk; t.ouldridge@imperial.ac.uk;

Abstract

Backbone-assisted assembly processes – such as protein folding – allow the assembly of a large number of structures with high accuracy from only a small handful of fundamental building blocks. We aim to explore general principles underlying this phenomenon by studying variants of the temperature-1 abstract tile assembly model (aTAM). We consider the existence of finite sets of tile types that can deterministically assemble any shape producible by a given assembly model; we call such tile type sets universal assembly kits. Our first model, which we call the “backboned aTAM”, generates backbone-assisted assembly by forcing tiles to be added to lattice positions neighbouring the immediately preceding tile, using a predetermined sequence of tile types. We demonstrate the existence of universal assembly kit for the backboned aTAM, and show that the existence of this set is maintained even under stringent restrictions to the rules of assembly. We hypothesise that the advantage of the backboned aTAM relative to the conventional aTAM – which does not possess such a set – is in part due to the specification of a sequence, and in part due to the geometric restrictions imposed by the backbone. To explore this intuition, we develop a second model call the “sequenced aTAM”. The sequenced aTAM uses a predetermined sequence of tiles, but does not constrain a tile to neighbour the immediately preceding tiles. We prove that this model has no universal assembly kit. The lack of such a kit is surprising,

given that the number of tile sequences of length N scales faster than the number of producible shapes of size N for a sufficiently large – but finite – set of tiles.

Keywords: self-assembly, abstract Tile assembly model, macromolecular folding

1 Introduction

1.1 Motivation and Aims

Molecular self-assembly, the process through which molecules adopt defined configurations in the absence of external control, is the foundation of biochemical complexity. The most basic form of self-assembly involves multiple subunits in solution spontaneously coming together to create a more complex structure, with that structure exclusively determined by the interactions between the subunits. The archetypal example is the joining of protein subunits to produce a larger quaternary structure (Greenbury et al. (2014)). Backbone-assisted assembly is a distinct process through which biology constructs complex structures. Here, the subunits are first assembled into a sequence connected by a backbone before folding into the final structure. Crucially, the sequence of subunits is not determined by the interactions between the subunits themselves. A quintessential example is the folding of polypeptide sequences into protein secondary and tertiary structures, with the sequence specified by an mRNA template (Anfinsen (1972)).

Backbone-assisted assembly allows control over which molecular building blocks are incorporated into a structure, and where. The consequences are evident in protein folding. Here, a large number of folded polypeptide structures are reliably selected from a vast space of possibilities, while utilizing only 20 amino acid subunits. If these same amino acids were instead assembled without first being polymerized into a sequence, the resultant structures would be non-specific (Sartori and Leibler (2020)). Conversely, if we did have a set of 20 building blocks that spontaneously formed a specific structure, then they would struggle to form alternative structures containing the same 20 basic subunits. In general, the spontaneous assembly of a large number of specific structures necessitates a number of building blocks that grows with the number of targets if specificity is to be maintained (Rothmund and Winfree (2000)).

With the advent of DNA nanotechnology, the last 20 years have seen the rise of synthetic systems capable of assembling into complicated structures (Rothmund (2006); Seeman and Sleiman (2017)). Although DNA itself is a copolymer of backbone-linked nucleotides, the key features of backbone-facilitated assembly are typically not explored in these systems. Many rely on the free assembly of short DNA oligonucleotide strands (Videbaek et al. (2022); Ke et al. (2012); Mohammed and Schulman (2013)). The technique of DNA origami (Rothmund (2006)) involves a long scaffold strand that is folded by short staples that bind to non-contiguous domains. These domains act like subunits embedded in a backbone chain, with their interactions mediated by the staples. However, with few exceptions (Young et al. (2020); Dunn et al. (2015)) the staples are intended to connect a unique pair of domains. Moreover, re-ordered

domains are not used to drive the formation of distinct, well-defined structures. The question of how a small number of basic units can direct the assembly of many distinct structures does not, therefore, arise.

Backbone-assisted assembly schemes could help to reduce assembly complexity in these synthetic systems by encoding a greater portion of the target structure through the backbone, reducing the number of subunits that must be fabricated. Progress in this space include developments in single-stranded nucleic acid nanotechnology (Shih et al. (2004); Geary et al. (2014); Zhou et al. (2020); Kočar et al. (2016); Han et al. (2017)) as well as alternative techniques such as programmable droplets (McMullen et al. (2022)). While promising, the sophistication of shapes accessible to existing systems is generally lower than those designed with conventional methods. A theory of backbone-assisted assembly could potentially aid in the development of more powerful artificial backbone-assisted assembly schemes.

While models of the backbone-assisted assembly exist (Lau and Dill (1989), Geary et al. (2019)), previous work hasn't focused explicitly on the backbone's importance relative to systems with no backbone, and existing models do not have straightforward non-backboned analogs for direct comparison. In this work, we develop a model based on the temperature-1 abstract Tile Assembly Model (aTAM), to build towards an understanding of general principles that give backbone-assisted assembly systems their unique advantages.

1.2 Review of aTAM

The aTAM is a model of computation via self-assembly (Rothemund and Winfree (2000)). The fundamental building blocks of the aTAM are tiles, with each face associated with a numbered glue. An aTAM instance is a tuple (T, g, A_0, τ) , where T is a set of tile types, g is a strength function that maps tuples of glue types onto integer values representing the strengths of their interaction. A_0 is a starting seed configuration (a set of tiles bound together in space) and τ is the temperature. Assembly occurs in discrete time steps, such that at each step, a tile is stuck onto the growing configuration. A tile can only be stuck onto the growing configuration if the sum of strengths of interactions formed between its glues and glues of the growing configuration meets or exceeds the temperature of the aTAM system.

For the purpose of studying assembly, it is natural to consider the number of tile types necessary to construct a particular shape deterministically, that is, without any chance of constructing off-target shapes. Existing work (largely on temperature-2 aTAM) generally considers scaled versions of shapes as equivalent (Soloveichik and Winfree (2007)), and the notion of a scaling factor, the scale at which some tile type set assembles a shape, arises as a result. By allowing shape scaling, the related concept of intrinsic universality arises. Intrinsic universality refers to the ability of an assembly scheme to not only assemble any shape, but simulate any other instance of the assembly scheme, in the sense of being able to replicate sequences of tile addition at some scale factor (Woods (2015)). The temperature-2 aTAM is known to be intrinsically universal (Doty et al. (2010); Demaine et al. (2012); Woods (2015)), whereas the temperature-1 aTAM is not intrinsically universal (Doty et al. (2011); Meunier and Woods (2017); Meunier et al. (2020)).

Intrinsic universality is a measure of the computational power of an assembly scheme. We have opted to use a different, but related, measure of the power of assembly schemes. We will consider whether particular assembly schemes admit a finite set of tile types that enable the deterministic assembly of all shapes achievable (achievable here means that there exists some input to the assembly system that constructs the given shape) by the given assembly scheme, and we call such a tile type set a **universal assembly kit**. In contrast to intrinsic universality, where non-trivial starting seeds are allowed, the definition of a universal assembly kit also explicitly disallows the use of any non-trivial starting seed. Further, we will be relying on assembly schemes which explicitly allow the rotation of tiles. These changes are consistent with our aims, as we are concerned with macromolecular assembly rather than using assembly for computation.

The existence of a universal assembly kit is weaker than intrinsic universality in the sense that such a set may not be able to simulate exact sequences of tile addition, but stronger in that shapes must be constructed at their exact scale. Since our models were developed from temperature-1 aTAM, we will be comparing results to the temperature-1 aTAM as a base. The non-existence of a universal assembly kit for the temperature-1 aTAM is provable via pumpability arguments on rectangles (Rothmund and Winfree (2000)). Algorithms do exist, however, for the minimization of tile type sets to deterministically construct particular shapes using variants of temperature-1 aTAM, via graph theoretic (Ahnert et al. (2010)) and boolean satisfiability (Russo et al. (2022); Bohlin et al. (2023)) approaches.

1.3 Summary of Results

We develop a model based on the temperature-1 aTAM that simulates a backbone-assisted assembly process, which we call the backboneed aTAM. We consider a variant of the aTAM that allows rotations (Demaine et al. (2012)) and for generality we allow mismatches to have negative strength, leading to mismatches that may block the addition of tiles (as in (Mañuch et al. (2009))). Like the base aTAM, the fundamental building blocks of our system are tiles with labelled faces. However, tiles can only be added in a specified order of tile types, and added tiles must neighbour the last added tile. The model can be thought of as mimicking idealized co-transcriptional folding; the added sequence information present in the backboneed aTAM means it can be more powerful at selectively producing specific shapes, allowing for a more repetitive use of tiles.

We provide here an informal definition of a **universal assembly kit** as this is vital to summarizing our results (a more thorough definition is presented in Section 3.1). Let an assembly scheme be a set of rules that constructs shapes from tiles with numbered faces and possible additional inputs (in our case, these additional inputs are usually a sequence in which tiles can be added). Then, a universal assembly kit is a finite set of tile types and interaction rules that allow any shape to be constructed deterministically, if that shape can be constructed at all by the assembly scheme (i.e. without imposing constraints on the set of tile types that may be used, some input to the assembly scheme exists that constructs the shape).

Our first main result is the existence of a universal assembly kit for the backboneed aTAM.

Theorem 1 A universal assembly kit for the backboneed aTAM exists.

The construction we arrive at to prove Theorem 1 is in some sense artificial as it relies exclusively on backbone routing to define shapes while disregarding non-backbone interactions. To circumvent this problem, and get closer to protein folding in which interactions with non-neighbouring amino acids are essential in determining the fold, we show that the existence of a universal assembly kit is preserved even when all adjacent tile faces are required to have attractive glue interactions. This finding recalls existing work on the aTAM, where mismatches and rotations were shown to have a weak effect on computational power (Mañuch et al. (2009)).

Theorem 2 A universal assembly kit for the backboneed aTAM exists such that the strength function g associated with the assembly kit does not encode any neutral interactions.

These two results contrast with the temperature-1 base aTAM, where a universal assembly kit does not exist (Rothemund and Winfree (2000)). To help us disentangle the effects of specifying a sequence and restricting the geometry of tile placement via a backbone, we develop a model we call the sequenced aTAM, where tiles are added in a predetermined sequence, as in the backboneed aTAM, but added tiles are no longer constrained to neighbor preceding tiles. While not reflective of any autonomous real world process, this construct serves as a null model for comparison to the backboneed aTAM. We find that unlike the backboneed aTAM, a universal assembly kit does not exist in the case of the sequenced aTAM.

Theorem 4 The sequenced aTAM does not admit a universal assembly kit.

This result is surprising given the known exponential scaling of the set of aTAM-producible shapes of a given size, since it is always possible to choose a finite tile set with a faster exponential scaling of the number of sequences of a given length (Klarner (1967)). Although this loss of a universal assembly kit is due to the loss of the geometric constraints imposed by the backbone, we cannot conclude that the presence of the backbone (in addition to the sequence) makes the backboneed aTAM more powerful than the sequenced aTAM. This complication arises because the backboneed aTAM has a smaller space of achievable shapes than the sequenced aTAM. Indeed, the sequenced aTAM can deterministically assemble any shape that can be assembled by the backboneed aTAM using a finite assembly kit (such a kit would be non-universal in the context of the sequenced aTAM). However, we have been unable to prove whether the sequenced aTAM can – like the backboneed aTAM – do so even when we impose no neutral interactions. We conclude by presenting some partial results in this direction.

2 Model Definitions

We begin with definitions borrowed from the aTAM literature (Rothemund and Winfree (2000); Doty et al. (2011)). We consider a variant of aTAM where tiles are allowed

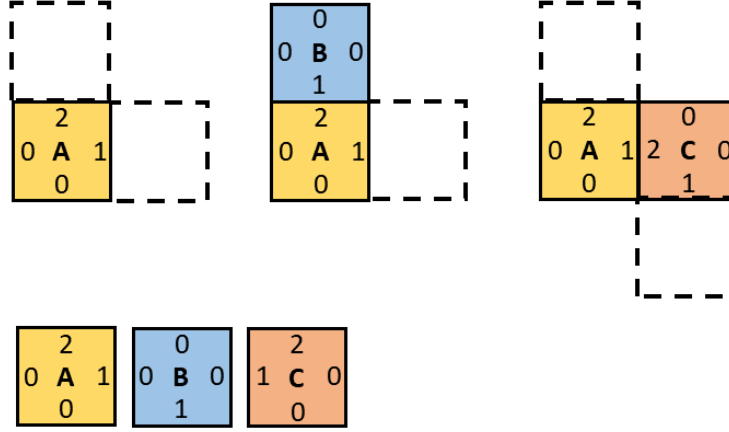


Fig. 1: A diagram illustrating aTAM assembly. The fundamental building blocks of assembly are square tiles with numbered faces. At each step, a tile drawing from the assigned set of tile types (**bottom**) is added to a random position neighbouring an existing tile, with the possible locations being restricted to those where the resulting sum of strengths of interactions formed is greater than or equal 1 (for temperature-1 aTAM). Here, the glue pair (1, 2) are predetermined to have strength of 1. Note that we use a variant of aTAM where tiles can be rotated. Example assembly steps starting from the state at the **top left** of the figure are given in **top centre** and **top right**.

to rotate (Demaine et al. (2012)). As tiles are allowed to rotate, we differentiate between an oriented tile, a 4-tuple of glue types $(\sigma_N, \sigma_E, \sigma_S, \sigma_W)$, and the orientation-free tile type which is an equivalence class of all cyclic permutations of any of its given tiles. In practice, the tile type can be associated with a default orientation, and the tile can be conceived of a tile type Θ placed in some specific orientation $\rho = \{N, E, S, W\}$ corresponding to the direction faced by the face that would face north in the default orientation.

A **configuration** is a partial function $A : \mathbb{Z}^2 \rightarrow \mathbb{T}$, where \mathbb{T} is the set of all possible tiles. $dom(A)$ is the set of points in configuration A with a tile. A coordinate $z \notin dom(A)$ is empty in A . A is a **subconfiguration** of A' if $dom(A) \subseteq dom(A')$. For convenience, we frequently use single-tile configurations $a = (\Theta, \rho, z)$ for a tile type Θ , an orientation ρ and a coordinate z , which we call **coordinated tiles**. The empty configuration is defined as A_{empty} such that $dom(A_{empty}) = \emptyset$. The addition of configurations $A'' = A + A'$ is well-defined if $dom(A) \cap dom(A') = \emptyset$, otherwise $A'' = \infty$ (Rothemund and Winfree (2000)). In the former case,

$$A''(z) = \begin{cases} A(z) & \text{if } z \in dom(A), \\ A'(z) & \text{if } z \in dom(A'). \end{cases}$$

The **strength function** is a partial function $g : \mathbb{Z}_+^2 \rightarrow \mathbb{Z}$. The strength function determines the type of interaction between two glues. Two glues σ and σ' have an attractive interaction if $g(\sigma, \sigma') > 0$, do not interact if $g(\sigma, \sigma') = 0$ (or have a neutral interaction) and have a repulsive interaction if $g(\sigma, \sigma') < 0$. Newly added tiles are allowed to form neutral or repulsive interactions, but only if the sum of interactions of each of their edges add up to greater than the temperature τ , which we have set equal to 1 for all the models that we consider.

The aim of any instance of an aTAM system is to produce shapes. For the base aTAM, shapes are assembled through the addition of tiles drawing from the tile type set T until no further tiles can be added (Refer to Figure 1 for an illustration, and reference (Rothmund and Winfree (2000)) for formal definitions). We describe as follows the way in which our two models, the **backboned aTAM** and the **sequenced aTAM** assemble their shapes.

We refer to the set of non-empty points $dom(A)$ as the **oriented shape** of a configuration A . We consider all outputs that can be transformed through rotations and translations as equivalent, hence we rely on a more general notion than oriented shape. A **shape** is thus an equivalence class of oriented shapes, containing oriented shapes that can be transformed to each other via rotations and translations, and the shape of a configuration is the shape to which its **oriented shape** belongs. We denote by \simeq the equivalence relation that defines a shape, such that if two oriented shapes S and S' have the same shape, then $S \simeq S'$. Hence, the only ambiguity in shape is overall rotation or translation, which do not violate the equivalence class.

Intuitively, the **backboned aTAM** aims to mimic a cotranslational folding system. Unlike the base aTAM, tiles can only be added in a predetermined order (a sequence of tile types is provided as an input to the assembly system), and any added tiles must neighbour the last added tile (Figure 2). Formally, a **backboned aTAM instance** is a 3-tuple (\mathcal{A}, Q, g) where \mathcal{A} is an initial configuration, Q is a sequence of tile types and g is a strength function.

Note that outside of specific theoretical constructs, \mathcal{A} is usually taken as the empty configuration, so that the backboned aTAM is normally conceived as a seedless assembly system. Compared to the base aTAM, the backboned aTAM accepts a sequence of tile types as opposed to a set of tile types as input. For the base aTAM, an operator $\rightarrow_{\mathbf{T}}^*$ was used to define the assembly of shapes. However, this is not an ideal descriptor for the backboned aTAM as it would obscure the contribution of the sequence. Rather, we build our definition from trajectories, which we define as follows:

Definition 1 A **trajectory** $\Psi = (A_0, A_1, A_2, \dots)$ is a sequence whose elements are either configurations or ∞ .

∞ is generally permitted only in the context of describing forbidden trajectories (that lead to two overlapping tiles).

A specific instance of the backboned aTAM can generate trajectories through the addition of tiles with types given by the sequence Q of the backboned aTAM system, while obeying the strength function g and rules about tile placement. A trajectory that can be generated by a backboned aTAM system is said to be complete with respect to the backboned aTAM system. We can now formally define a complete trajectory.

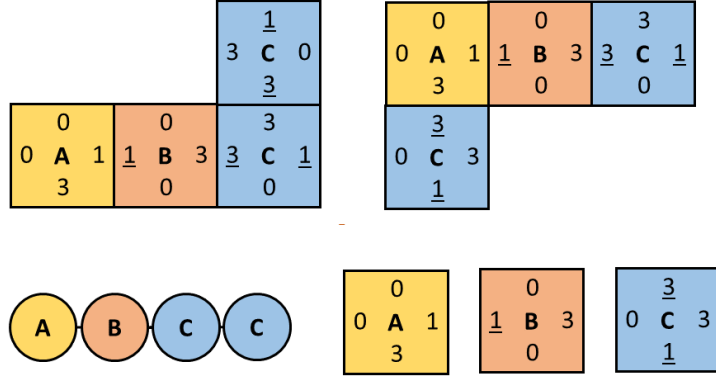


Fig. 2: A figure illustrating assembly via the backboneed aTAM and the sequenced aTAM. Consider an instance (A_{empty}, Q, g) of either the backboneed aTAM or the sequenced aTAM, and where $g(x, x) = 1$. An example sequence Q is provided in the **bottom left**, with the letters of each tile type corresponding to tiles found in the **bottom right**. For a backboneed aTAM instance, added tiles must neighbour the tile added in the immediately preceding step, and hence only the **top left** configuration can result from the backboneed aTAM. By contrast, the sequenced aTAM has no such restriction, and both top left and top right configurations can be the final configuration in a trajectory of a sequenced aTAM instance.

Definition 2 Consider a backboneed aTAM instance (\mathcal{A}, Q, g) , with the sequence of tile types $Q = (\Theta_1, \Theta_2, \dots, \Theta_\omega)$. A trajectory $\Psi = (A_0, A_1, A_2, \dots)$ is said to be complete with respect to (\mathcal{A}, Q, g) if the following hold.

1. Starting configurations are consistent, that is $A_0 = \mathcal{A}$.
2. $A_t = A_{t-1} + a_t$ with a_t chosen randomly under the constraints:
 - (a) $A_t \neq \infty$ for any t
 - (b) a_t is the coordinated tile formed by Θ_t after undergoing some rotation and placed on a coordinate z .
 - (c) Any coordinated tile in A_t is such that the sum of strengths $\sum_i g(\sigma_i, \sigma'_i)$, where σ_i is the face i of the tile, σ'_i is the tile face adjacent to σ_i and $g(\sigma_1, \sigma'_1) = 0$ if σ'_i belongs to an empty coordinated tile (A configuration A_t that obeys this assumption for some interaction function g is called **g-valid**).
 - (d) Each added coordinated tile a_t forms an attractive interaction with the coordinated tile a_{t-1} added in the last time step unless $t = 0$ or A_{t-1} is empty.
3. The trajectory terminates upon reaching A_ω or when no such single tile configuration a_t can be added. In the latter case, the trajectory is said to have been prematurely terminated.

By this definition, the first tile added in an empty configuration can be placed in any coordinate, at any orientation. The set of assembled configurations for an instance

of the backboneed aTAM is defined as the set containing all terminal configurations for all complete trajectories generated by the backboneed aTAM instance. The set of assembled shapes for a backboneed aTAM instance is thus the set containing all shapes of assembled configurations of the backboneed aTAM instance.

We further define a model that we call the sequenced aTAM, which serves as a null model against which features of the backboneed aTAM can be compared. The definition of a sequenced aTAM instance, along with the definition of its complete trajectories, are as follows. A **sequenced aTAM instance** is a 3-tuple (\mathcal{A}, Q, g) (and hence it has identical descriptors to a backboneed aTAM instance). The key difference lies in the definition of a complete trajectory for the sequenced aTAM, which does not mandate that tiles are placed adjacent to the previous tile.

Definition 3 Consider a sequenced aTAM instance (\mathcal{A}, Q, g) , with the sequence of tile types $Q = (\Theta_1, \Theta_2, \dots, \Theta_\omega)$. A trajectory $\Psi = (A_0, A_1, A_2, \dots)$ is said to be complete with respect to (\mathcal{A}, Q, g) if the following hold.

1. Starting configurations are consistent, that is $A_0 = \mathcal{A}$.
2. $A_t = A_{t-1} + a_t$ with a_t chosen randomly under the constraints:
 - (a) $A_t \neq \infty$ for any t .
 - (b) a_t is the coordinated tile formed by Θ_t after undergoing some rotation and placed on a coordinate z .
 - (c) Any coordinated tile in A_t is such that the sum of strengths $\sum_i g(\sigma_i, \sigma'_i)$, where σ_i is the face i of the tile, σ'_i is the tile face adjacent to σ_i and $g(\sigma_1, \sigma'_1) = 0$ if σ'_i belongs to an empty coordinated tile (A configuration A_t that obeys this assumption for some interaction function g is called **g-valid**).
3. The trajectory terminates upon reaching A_ω or when no such single tile configuration a_t can be added. In the latter case, the trajectory is said to have been prematurely terminated.

We end this section by defining a few ideas necessary to build towards a notion of a universal assembly kit. The set of all shapes that are defined by terminal configurations in any instance of an assembly model (the backboneed or sequenced aTAM) is called the **shape space** of assembly model; informally, it is the set of shapes that can be assembled by the model, allowing any sequence and strength function. A given instance of the backboneed or sequenced aTAM, with a specific sequence and strength function, is called **deterministic** if and only if its set of assembled shapes contains exactly one element. We use **oriented determinism** to refer to the stronger condition of a system assembling only a single oriented shape (the latter is only possible if the starting configuration is non-empty).

3 Results

3.1 The Backboneed aTAM admits a Universal Assembly Kit

Our results are concerned with finding, for both the backboneed and sequenced aTAM, a finite tile type set and corresponding strength function that allows the deterministic

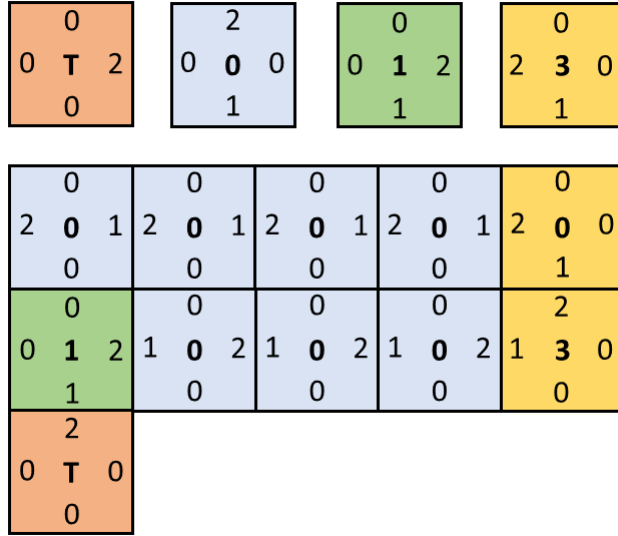


Fig. 3: A figure illustrating a finite set of “directed” tiles that comprise a universal assembly kit of the backboneed aTAM (**top**), as well as an example configuration utilizing these tiles (**bottom**).

assembly of any shape within the shape space of the model. Here, the starting configuration must be empty set and the sequence of tiles can be arbitrary, within those sequences permitted by the finite tile set. We call such a tile type set a **universal assembly kit**. We begin our results with the following Lemma.

Lemma 1 *The shape space of the backboneed aTAM is a subset of the shapes of self-avoiding paths.*

Proof This lemma trivially proceeds from definition 2, as added tiles must neighbour the last added tile. \square

Theorem 1 *A universal assembly kit for the backboneed aTAM exists.*

Proof Since any shape that can be assembled by a backboneed aTAM system is a shape of some self-avoiding walk, we can always assemble any shape (achievable by a backboneed aTAM system) by encoding the set of left, right or forward moves of the underlying self-avoiding walk. We use glues 0, 1 and 2, along with the following strength function:

$$g = \begin{cases} 1, & \text{if } (\sigma, \sigma') = (1, 2) \text{ or } (\sigma, \sigma') = (2, 1), \\ 0, & \text{otherwise,} \end{cases} \quad (1)$$

Then, each left, right or forward move can be performed by a specific “directed” tile, shown in Figure 3. An additional tile encoding the start of the shape is required, but there is no need for an end tile as any of the directed tiles can be placed at the end of any self-avoiding walk without impacting the final shape. Hence, a universal assembly kit with 4 tiles is sufficient

to assemble any shape achievable by the backboneed aTAM, without requiring a starting seed configuration or needing to scale up the shape. \square

Given this theorem, the following corollary trivially holds.

Corollary 1 *The shape space of the backboneed aTAM is equal to the set of shapes of self-avoiding paths.*

Proof Any self-avoiding path can be constructed using the method in Theorem 1. \square

These initial results are fairly straightforward. However, the construct we have arrived at is somewhat artificial when considering the physical system being emulated (co-translational folding), since the shape is completely determined by the backbone routing and non-backbone-adjacent interactions are irrelevant. This result is only possible due to the use of neutral interactions, or by allowing adjacent tiles to have weak repulsive interactions (that are not sufficiently strong to prevent the addition of a tile). We now consider, therefore, whether the existence of a universal assembly kit is maintained even if we require that all inter-tile interactions in any configuration are attractive, so that neighbours that are brought together by the folded pathway must interact attractively.

Theorem 2 *A universal assembly kit for the backboneed aTAM exists such that all inter-tile interactions in any configuration are required to be attractive.*

Proof The existence of some infinite tile set is trivial, as in the construction of all possible shapes, one can use the tile set in Theorem 1, but replace all glue types of all faces that neighbour another tile face with some unique attractive glue type. However, a universal assembly kit requires a finite number of tiles and reusing the same attractive glue type multiples times within a configuration can result in non-deterministic assembly as tiles can be attracted into incorrect positions (Figure 4). Hence, we must proceed to construct a scheme for numbering tile types such that only a finite number of glue types N are required while still guaranteeing deterministic shape assembly. Let the glue types be labelled $\{0, 3, 4, 5, \dots, N-1\}$, and let the strength function g be defined as follows.

$$g(\sigma, \sigma') = \begin{cases} 1, & \text{if } (\sigma, \sigma') = (1, 2) \text{ or } (\sigma, \sigma') = (2, 1) \text{ or } (\sigma = \sigma' \text{ and } \sigma > 2), \\ -3, & \text{otherwise.} \end{cases} \quad (2)$$

For this $g(\sigma, \sigma')$, interactions are either attractive or so repulsive that they would preclude tile placement. In any configuration formed by this tile set, all interactions must therefore be attractive, as required.

We call the fundamental tile types for our construction “interacting directed tile types”, and define them as follows.

Definition 4 Consider the following set of tile types:

1. $\hat{\Theta}_T(\sigma, \sigma', \sigma'') = (2, \sigma, \sigma', \sigma''), \sigma, \sigma', \sigma'' = 0, 3;$
2. $\hat{\Theta}_0(\sigma, \sigma') = (2, \sigma, 1, \sigma'), \sigma, \sigma' = 0, 3, 4, 5, \dots, N-1;$
3. $\hat{\Theta}_1(\sigma, \sigma') = (2, 1, \sigma, \sigma'), \sigma, \sigma' = 0, 3, 4, 5, \dots, N-1;$
4. $\hat{\Theta}_3(\sigma, \sigma') = (2, \sigma, \sigma', 1), \sigma, \sigma' = 0, 3, 4, 5, \dots, N-1;$
5. $\hat{\Theta}_H(\sigma, \sigma', \sigma'') = (1, \sigma, \sigma', \sigma''), \sigma, \sigma', \sigma'' = 0, 3, 4, 5, \dots, N-1.$

We describe these tile types as **interacting directed tile types** (Figure 5).

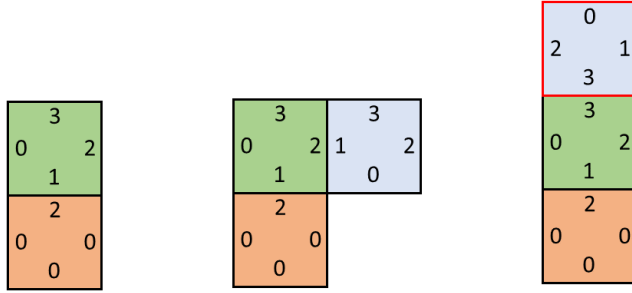


Fig. 4: A figure illustrating the difficulties associated with assembly without neutral interactions. While in principle one can replace the neutral interface type 0 with a self-attractive interface type 3, such attractive interfaces can pull tiles towards unintended positions (**right**).

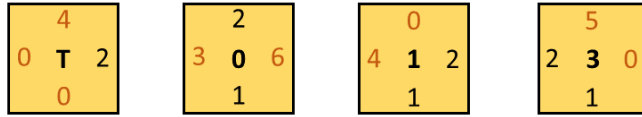


Fig. 5: Example interacting directed tiles, with red/brown glue types representing σ , σ' or σ'' and black glue types representing backbone faces.

These tile types are constructed by analogy with the tile types used in the proof of Theorem 1. For example, $\hat{\Theta}_0$ is a set of tile types with glue types 1 and 2 (**backbone glue types**) in the same pattern as tile type 0 in Fig. 3, but with variable glues on the other faces; $\hat{\Theta}_0(\sigma, \sigma')$ identifies a specific member of that set. Non-backbone glue types are divided into zero and non-zero types; we denote by $B^c(\Theta)$ the set of non-zero, non-backbone glue types on tile type Θ . Tile faces endowed with backbone and non-backbone glue types are correspondingly called **backbone faces** and **non-backbone faces**, respectively.

We present an algorithm for selecting a sequence Q , using a subset of the tiles from Definition 4 with $N = 7$, to define a backbone aTAM system (\mathcal{A}, Q, g) that can deterministically assemble any given shape within the shape space of the backbone aTAM. The interacting directed tile types in Definition 4, along with the strength function in Equation 2, therefore define a universal assembly kit for the backbone aTAM, proving the existence of such a kit by construction.

Let $\Psi = (A_{\text{empty}}, A_1, \dots, A_\omega)$ be a complete trajectory that assembles a shape \bar{S} , defining an arbitrary Hamiltonian path through the shape. A sequence of backbone faces consistent with this trajectory can then be selected as in the proof of Theorem 1, fixing whether each tile in the sequence is drawn from the set $\hat{\Theta}_T$, $\hat{\Theta}_0$, $\hat{\Theta}_1$, $\hat{\Theta}_3$ or $\hat{\Theta}_H$. Hence, we only need to select the non-backbone interactions of tile types in the sequence in such a way as to ensure deterministic production of the desired shape.

Assume that the subtrajectory $(A_{\text{empty}}, A_1, \dots, A_{t-1})$ is given, and that we wish to obtain the next coordinated tile a_t such that $A_t = A_{t-1} + a_t$. We apply the following rules to select the non-backbone faces of a_t and hence specify Θ_t , the t th tile type in the sequence Q :

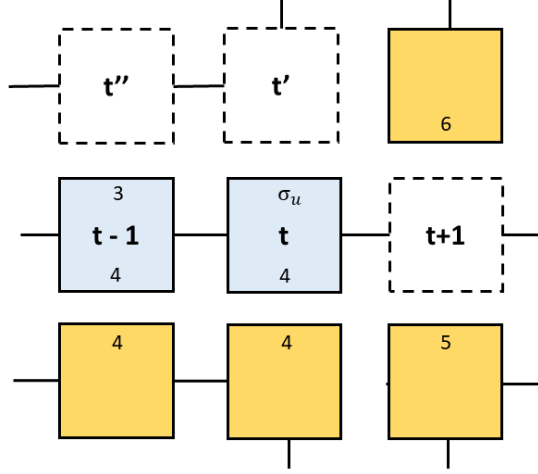


Fig. 6: An illustration of the inequalities on the faces of tiles when constructing an assembly kit for the backboneed aTAM without neutral interactions. After setting the glue types of known faces, there remains one face with unknown glue type σ_u . $\sigma_u \neq 3$, $\sigma_u \neq 5$ and $\sigma_u \neq 6$, so $\sigma_u = 4$ is the only correct option if we restrict ourselves to 4 attractive non-backbone glue types.

1. Non-backbone faces of a_t with a neighbour in A_t are made to match their neighbouring glue type.
2. Non-backbone faces of a_t with no neighbour in A_ω (the terminal configuration of Ψ) are assigned the repulsive glue type 0.
3. Non-backbone faces of a_t with no neighbour in A_t but with a neighbour in A_ω are assigned an unknown glue type σ_u .
4. If the coordinated tile a_t has two (or more) unknown glue types σ_u and σ'_u , then set $\sigma_u = \sigma'_u$.

There are two sets of inequalities that must be fulfilled by σ_u (see example in Figure 6):

1. Define by $\tilde{B}^c(a_{t-1}, A_{t-1}) \subseteq B^c(\Theta_{t-1})$ the set of non-backbone, non-zero glue types of a_{t-1} assigned to at least one face of a_{t-1} with an empty adjacent position in A_{t-1} . Then, $\sigma_u \notin \tilde{B}^c(a_{t-1}, A_{t-1})$ to stop a tile with type Θ_t binding to a_{t-1} in the incorrect location.
2. Define by $M(a_{t+1}, A_{t+1})$ the set of non-backbone, non-zero glue types of faces adjacent to a_{t+1} in A_{t+1} . Then, $\sigma_u \notin M(a_{t+1}, A_{t+1})$ to stop a tile with type Θ_{t+1} binding to a_t incorrectly.

Our construction means that $\tilde{B}^c(\Theta_{t-1})$ has at most 1 member, while lattice placement rules mean that $M(a_{t+1}, A_{t+1})$ has at most 2 members, since the next tile can only have two non-backbone-connected neighbours. Hence, there are at most 3 inequalities on the sole unassigned glue type σ_u , and hence 4 attractive glue types are always sufficient to ensure that σ_u has an assignment that allows deterministic production of the desired shape. A worst-case scenario is illustrated in Figure 6.

The arguments above break down for the penultimate tile as the final tile can have three non-backbone-connected neighbours. However, in this case all of the final neighbours of a_ω and $a_{\omega-1}$ are already in place. Therefore the non-backbone glue types of $a_{\omega-1}$ are either specified by neighbouring tiles that are present in the configuration $A_{\omega-1}$, or 0. They cannot, therefore, cause any ambiguity when a_ω is placed, with glue types set either to match neighbours present in configuration A_ω , or 0. Taking $N = 7$, 208 tiles are defined by Definition 4. This number provides an upper bound on the size of the minimal universal assembly kit for the backboneed aTAM. \square

This result again contrasts with the base aTAM, for which a universal assembly kit does not exist. Hence, in some sense, backbones increase our ability to reliably assemble a complex structure from a small set of subunits.

3.2 Tile Complexity Comparisons between the Backboneed and Base aTAM

As well as considering universal assembly kits, we may also ask whether the backboneed aTAM requires fewer unique tiles (that is, has a lower **tile complexity**) to deterministically produce a single target shape than the base temperature-1 aTAM. For large enough target shapes, the argument in Section 3.1 suggests that the backboneed aTAM will incur a smaller tile complexity, as the tile complexity for a specific target is upper-bounded by the universal kit of size 208, whereas we expect tile complexity to grow indefinitely with the target shape size for the base aTAM (Rothemund and Winfree (2000)).

We can apply the method in (Ahnert et al. (2010)) to upper bound a minimal tile complexity for a given shape for the base aTAM, and we can apply the algorithm constructed in Theorem 2 to find an upper bound on the tile complexity required to assemble the same shape using the backboneed aTAM. In Fig. 7, we plot the difference in these upper bounds on the tile complexity for a single target shape, as a function of shape size. We consider both rectangular target shapes, and rectangles with a bulge to produce a target with lower symmetry. In this case, the Hamiltonian path taken by the backbone is assumed to zig-zag down the rectangle along each row starting from the top row of the rectangle (Figure 7 (a) and 7 (b)).

As can be seen in Figure 7, the bounds suggest that the very smallest rectangles can be constructed with fewer unique tile types using the base aTAM compared to the backboneed aTAM. This fact is likely because unbackboned assembly is better able to take advantage of the symmetry present in a rectangle (Greenbury et al. (2014)), whereas the backboneed aTAM is an inherently asymmetric assembly method. As expected, the asymmetric bulged rectangles display no such behaviour as they have no symmetries that base aTAM can take advantage of. For larger rectangles, the backboneed aTAM becomes more efficient than the base aTAM due to its ability to use the same tile types in locations with distinct symmetry, and does so well before the bound of the universal kit size is reached.

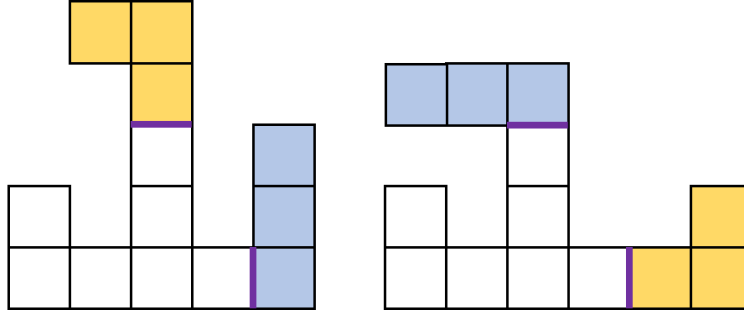


Fig. 8: Intuition for Lemma 2. **(Left)** A configuration A given some starting configuration A_0 (white), and subconfigurations A_ϵ (blue) and $A_{\epsilon'}$ (yellow). **(Right)** Assume the faces in purple have the same glue, then subshapes that grow from the purple faces can be flipped while maintaining the same tile type sequence Q , forming an alternate configuration A' .

except added tiles are no longer constrained to neighbour immediately preceding tiles. We will see that no universal assembly kit exists that allows the sequenced aTAM to deterministically assemble every shape in its shape space, even when allowing for neutral faces.

Our proof proceeds from the following intuition. For an instance of the sequenced aTAM, shapes that grow from a face of a configuration A_t for times $t' > t$ are encoded fully by the glue of the face and the tile type sequence past past time t (if we ignore the ‘blocking’ of growth by preexisting tiles). Hence, if we have two tile faces with the same glue type at a time t , then (ignoring tile blocking), we cannot stop a shape that grows from one of the faces from also growing on the other face (Figure 8). Hence, if we need to grow N different shapes from N different faces at a time t , we require at least N different glue types. If the growth of certain shapes requires an arbitrarily large number of open faces, $N \rightarrow \infty$, then a finite universal assembly kit will be impossible.

This intuition is incomplete for the following reasons:

1. We haven’t considered the effect of tile blocking, which can potentially allow many different shapes to grow from the same glue, based on the blocking pattern.
2. We haven’t shown that, for certain classes of shapes, a large number of open faces are unavoidable. A requirement for a large number of open faces is not trivial. For example, when constructing rectangles of any size, it is possible to avoid opening more than two non-neutral faces at any one time by constructing the rectangle row-wise.

Lemma 2 formalizes this intuition. Using this lemma, Theorem 3 in the main text builds a set of assumptions that allow us to avoid tile blocking and forces us to ‘open’ at least N distinct glue types when $g \geq 0$. This result is extended to unrestricted g in Theorem 6 in the appendix. We then develop a class of shapes that obey these assumptions for arbitrarily large N in Definition 6, and complete the proof in Theorem 4.

We first state a few additional definitions to aid in our proof. Let the **face coordinate** (z, k) for a 2D coordinate z and orientation $k \in \{N, E, S, W\}$ denote the k -facing face of the coordinate z . Then, let $A(z, k)$ return the glue type of (z, k) . Two configurations A and A' are **adjacent** if there exist $z \in \text{dom}(A)$ and $z' \in \text{dom}(A')$ such that z neighbours z' . It is always possible to define a **face set** of a configuration $\text{face}(A)$ as the set of faces of all coordinates in $\text{dom}(A)$. Two neighbouring faces (z, k) and (z', k') form a **face-pair**. Two configurations A and A' are said to be **uniquely adjacent** through a face-pair $((z, k), (z', k'))$ if it is the only face-pair where one face of the pair is in the face set of each configuration.

Over the course of our proofs, we will be relying on sufficient and necessary conditions for some configuration A_t to be part of a complete trajectory. We note that from the definitions of the backbone and sequenced aTAM, it is clear that g -validity is a necessary condition for any configuration in a complete trajectory. Together with the consistency of starting configurations and added tiles matching the sequence Q (either to the end of Q or until the point of premature termination), g -validity becomes sufficient in ensuring that a given trajectory is complete. We now proceed by formalizing our intuition that open faces growing distinct subshapes require distinct faces, under some set of assumptions:

Lemma 2 *Consider a sequenced aTAM instance $\mathcal{P} = (A_0, Q, g)$. Let the following be true:*

1. *Let $A_0(z_\epsilon, k_\epsilon) = A_0(z_{\epsilon'}, k_{\epsilon'})$ for two faces (z_ϵ, k_ϵ) and $(z_{\epsilon'}, k_{\epsilon'})$.*
2. *Let A_ϵ be a configuration adjacent to A_0 uniquely through face pair $(\dot{e}_\epsilon, \ddot{e}_\epsilon)$ (\dot{e}_ϵ in A_ϵ and \ddot{e}_ϵ in A_0), while $A_{\epsilon'}$ is a configuration adjacent to A_0 uniquely through face pair $(\dot{e}_{\epsilon'}, \ddot{e}_{\epsilon'})$ and assume A_ϵ and $A_{\epsilon'}$ are not adjacent to each other. Assume further that some complete trajectory $\Psi = (A_0, A_1, A_2, \dots, A_\omega)$ generated by T exists such that $A_\omega = A_0 + A_\epsilon + A_{\epsilon'} + A_c$ for some arbitrary configuration A_c not adjacent to A_ϵ or $A_{\epsilon'}$.*
3. *Let $A_{\epsilon \rightarrow \epsilon'}$ be an affine transformation of A_ϵ that maps \dot{e}_ϵ to $\dot{e}_{\epsilon'}$, and similarly for $A_{\epsilon' \rightarrow \epsilon}$. Then, assume that $A'_\omega = A_0 + A_{\epsilon \rightarrow \epsilon'} + A_{\epsilon' \rightarrow \epsilon} + A_c$ is g -valid.*

Then, there exists another trajectory $\Psi' = (A'_0, A'_1, \dots, A'_\omega, \dots)$ complete with respect to \mathcal{P} such that the terminal configuration of Ψ' is A'_ω or has A'_ω as a subconfiguration.

Proof We show that some selection of A'_t for Ψ' meets the definition of a complete trajectory. First, by setting $A_0 = A'_0$, starting configuration consistency is established. Configurations in the trajectory Ψ can be decomposed as $A_t = A_0 + A_{\epsilon, t} + A_{\epsilon', t} + A_{c, t}$, where $A_{x, t}$ is a subconfiguration of A_x (present at time t). We require that it is possible to construct a trajectory Ψ' complete with respect to T , such that each entry $A'_t = A_0 + A_{\epsilon \rightarrow \epsilon', t} + A_{\epsilon' \rightarrow \epsilon, t} + A_{c, t}$ up to $t = \omega$ is g -valid. This is always true at $t = 0$, and tile addition at time $t + 1$ (following the tile type sequence Q) can always result in a g -valid $A'_{t+1} = A_0 + A_{\epsilon \rightarrow \epsilon', t+1} + A_{\epsilon' \rightarrow \epsilon, t+1} + A_{c, t+1}$ up to $t + 1 = \omega$. Since the order of tiles added also matches the sequence Q , the condition for complete trajectories of sequence aTAM is obeyed, and the theorem is thus true by induction. \square

In essence, we have made the general argument that if the left hand configuration in Fig. 8 is complete with respect to T , and swapping over the yellow and blue sub-configurations does not result in a clash, then the right hand configuration can also be formed under the dynamics of T .

Some additional definitions will be useful at this point as we leverage Lemma 2 to show that deterministic growth of certain shapes with M protrusions from an initial subshape requires at least $\frac{M}{4}$ unique tiles. Let an **open face** be a face of some non-empty tile in a configuration that neighbours an empty face, and glue types belonging to some open face are similarly known as open glue types. Let $\mathbf{E}(\mathbf{A})$ return the oriented shape of a configuration.

Theorem 3 Consider an oriented shape $S = \bigcup_{i=0}^M S_i$ such that:

1. For any $i, j \in 1, \dots, M$, $S_i \not\cong S_j$ for any $i \neq j$. That is, each S_i is distinct up to rotations and translations.
2. For any $i, j \in 1, \dots, M$, S_i has no point that neighbours any point in any other S_j where $i \neq j$.
3. For any $i \in 1, \dots, M$, S_i has exactly one coordinate that neighbours a coordinate in S_0 , and S_0 has exactly one coordinate that neighbours this coordinate. We denote by \check{z}_i the coordinate in S_i and by \check{z}_i the neighbouring coordinate in S_0 (neighbouring faces are similarly labelled $(\check{z}_i, \check{k}_i)$ and $(\check{z}_i, \check{k}_i)$).
4. S and S_0 are not rotationally symmetric. Additionally, there does not exist S_t , a subshape of S , such that $S_t \neq S_0$ but $S_t \simeq S_0$.

Consider a sequenced aTAM instance $\mathcal{P} = (A_0, Q, g)$ such that $E(A_0) = S_0$ and **the range of g is restricted to $g \geq 0$** . If assembly is deterministic and the terminal configuration A_ω is such that $E(A_\omega) = S$ as defined above, then the number of unique tile types required in A_0 grows with at least $\frac{M}{4}$.

Proof Condition 4 and determinism imply that \mathcal{P} is oriented-deterministic. Assume A_0 has fewer than M distinct open glue types, so some S_i and S_j must be anchored at glues of the same type. Then, Theorem 2 implies one of the following must be true:

1. $S_i \simeq S_j$.
2. An overlap of configurations occurs when transforming the configurations neighbouring the two faces $(\check{z}_i, \check{k}_i)$ and $(\check{z}_j, \check{k}_j)$ (in the language of Theorem 2, $A'_\omega = \infty$ and is thus not g -valid).

Each of these possibilities leads to a contradiction. The first possibility directly contradicts condition 1. The second possibility results in some point of S_i (or S_j) neighbouring some additional point in S outside of S_i (or S_j), contradicting condition 2 or 3. Hence, by contradiction, A_0 must have M or more open faces. As each tile type has at most 4 unique faces, the number of unique tile types in A_0 must grow with at least $\frac{M}{4}$. \square

The bolded restriction on g in Theorem 3 excludes the possibility of repulsive interactions. Thus we do not have to consider situations where a tile is blocked by some repulsive interaction, rather than overlapping. We have chosen to include this simplified form of the theorem in this text as it provides a better intuition for our proof. However, with a few additional assumptions, we show how this restriction can be lifted in Theorem 6, included in Appendix A, and the remainder of our results are consistent with this more general form.

We now construct a class of target shapes such that shapes obeying the assumptions in Theorem 3 (and more strongly, those in Theorem 6) cannot be avoided in the

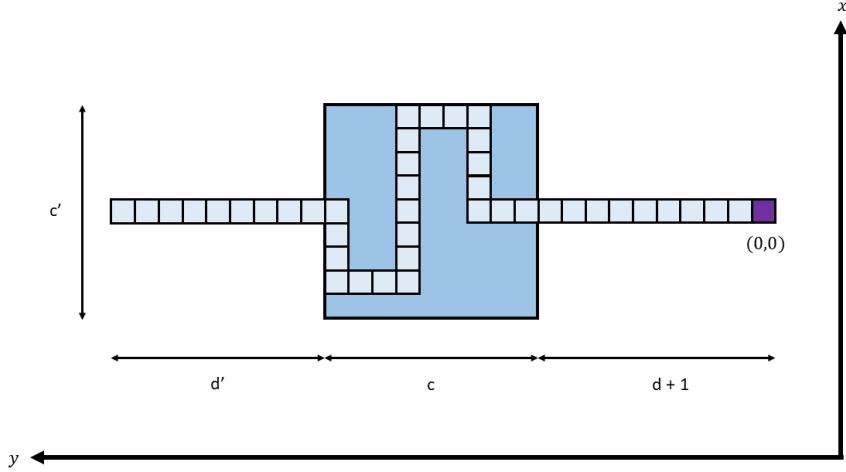


Fig. 9: An oriented shape W belonging to the set $\mathbb{W}_{9,9,9,9}$. The **start point** of the oriented shape is given in purple. The dark blue shaded box is the **canvas** of W , the region of W containing an arbitrary self-avoiding walk.

assembly of these targets. To do so, we define a **branching point** as any coordinate of some oriented shape S with three or more neighbours in S , while a **corner** is a coordinate in S with two neighbours in S , such that the corner and its two neighbours do not form a straight line. Then, let a **straight line segment** be a line starting at some branching point or corner, and ending at the next branching point/corner. The **distance** between two points (x_1, y_1) and (x_2, y_2) is taken to be $|x_2 - x_1| + |y_2 - y_1|$. We can now begin describing the fundamental components of our constructed target shape.

Definition 5 An oriented shape W is in the set $\mathbb{W}_{d,c,c',d'}$ for arbitrary positive integers d, c and d' and odd positive integer c' if:

1. It is a 2-Dimensional self-avoiding walk constrained to a length of c' in one dimension and a length of $d + c + d'$ in the other dimension. Irrespective of the true orientation of the walk in the 2D plane, c' is called the width of the oriented shape (with corresponding dimension called the width dimension) and $d + c + d'$ is called the height of the shape (with corresponding dimension called the height dimension).
2. The first $d + 1$ and last d' coordinates (along the height dimension) form straight lines that, if extended, would cut through centre of the central $c \times c'$ rectangle, called the canvas.
3. The canvas contains some self-avoiding walk that doesn't leave the canvas and connects the two straight lines.

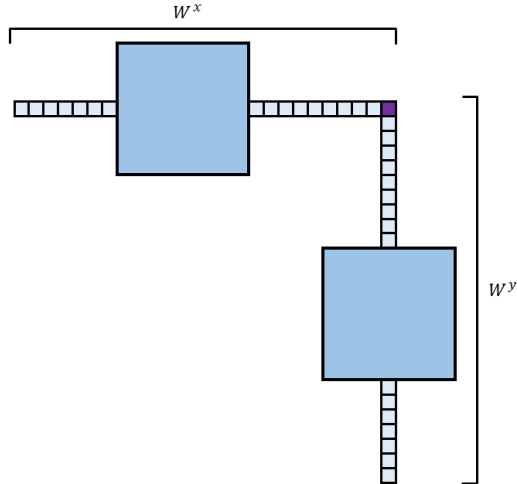


Fig. 10: An oriented shape R belonging to the set \mathcal{R}_9^0 , consisting of W^x a horizontally aligned member of $\mathbb{W}_{9,9,9,7}$ joined with W^y a vertically aligned member of $\mathbb{W}_{9,9,9,7}$. Shaded blue boxes represent canvas regions of constituent walks. Each of these boxes are constrained to contain distinct self-avoiding walks.

4. Any point in W is of at least distance 3 from any other point in W , except for the 2 points immediately preceding it and the 2 points immediately succeeding it along the walk.
5. Any straight line segments in the walk W must be of at least length 4.

Refer to figure 9 for an example of an oriented shape in $\mathbb{W}_{d,c,c',d'}$.

Note that features 3 and 4 are not necessary for Theorem 3, but are necessary for the target shape we are constructing to obey the assumptions of Theorem 6. We use these oriented shapes to build larger oriented shapes with the aim of creating a class of shapes that fulfill the assumptions laid out in Theorem 3 (as well as Theorem 6). We call these larger oriented shapes treeangles, and we define them as follows.

Definition 6 A *treeangle* of order V with fundamental length L is an oriented shape S that can be constructed as follows.

1. An oriented shape in the set \mathcal{R}_L^0 can be constructed by placing a horizontal oriented shape (height dimension along x) $W^x \in \mathbb{W}_{L,L,L,L-2}$ and a vertical oriented shape (height dimension along y) $W^y \in \mathbb{W}_{L,L,L,L-2}$ next to each other, with the two connected at their start points (Figure 10).
2. Given the Definition for \mathcal{R}_L^0 , \mathcal{R}_L^1 can be constructed by connecting a horizontally aligned $W^x \in \mathbb{W}_{L,L,L,L}$ with a vertically aligned $W^y \in \mathbb{W}_{L,L,L,L}$, and then connecting two newly sampled oriented shapes from \mathcal{R}_L^0 at the endpoints of W^x and W^y (Figure 11).

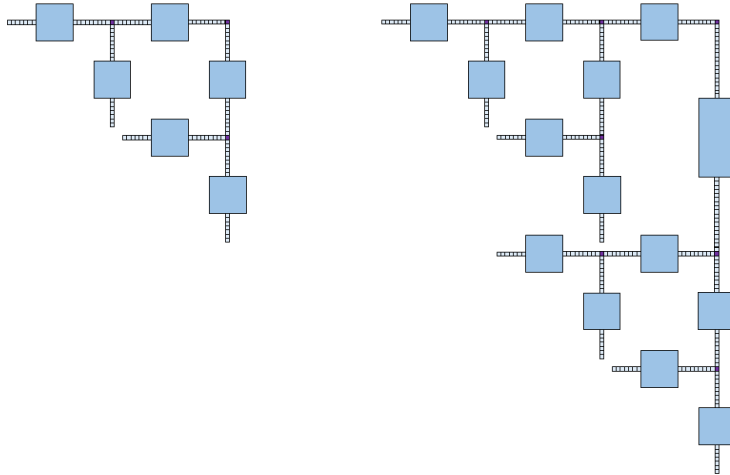


Fig. 11: Oriented shapes R_1 (left) and R_2 (right) belonging to \mathcal{R}_9^1 and \mathcal{R}_9^2 respectively. Oriented shapes in \mathcal{R}_9^2 can be obtained starting from two oriented shapes in \mathcal{R}_9^1 by joining them via a horizontal walk $W^x \in \mathbb{W}_{9,9,9,9}$ and a vertical walk $W^y \in \mathbb{W}_{18,19,9,18}$. Shaded blue boxes represent canvas regions containing distinct self-avoiding walks.

3. For higher orders v , \mathcal{R}_L^v is obtained in a similar way from \mathcal{R}_L^{v-1} . However, to ensure that the oriented shapes fit in the 2D lattice, $W^y \in \mathbb{W}_{2^{v-1}L, 2^{v-1}L+2^{v-1}-1, L, 2^{v-1}L}$ (Figure 11).
4. To construct a treeangle S , sample two oriented shapes R_V and \hat{R}_V from \mathcal{R}_L^V . \hat{R}_V is horizontally flipped and translated, forming \hat{R}_V and $I \in \mathbb{W}_{2^{v-1}L, 2^{v-1}L+2^{v-1}-1, L, 2^{v-1}L}$ is sampled to connect R_V and \hat{R}_V (Figure 12).
5. During construction, every walk sampled from some $\mathbb{W}_{d,c,c',d'}$ is sampled without replacement. That is, each section of the treeangle (defined as any contiguous path between two branching points) has a unique walk.
6. A shape \bar{S} consisting of rotations and translations of some (oriented) treeangle S is also known as a treeangle. The order and fundamental length of \bar{S} are equal to the order and fundamental length of S .

Using the treeangle, we can now set out to prove the inexistence of a universal assembly kit for the sequenced aTAM. Before doing so, we lay out a few final definitions. Let $\mathbf{G}_S(\mathbf{S})$ return a graph whose vertices represent coordinates of S , and where edges are drawn between neighbouring coordinates. Let a **terminal branching point** be a branching point v such that a path P on the graph $G_S(S)$ can be drawn from some leaf node (a node with only one edge in a graph) to v such that P contains no other branching point (that is, it a branching point where at least one of the paths from it to an end of the branch includes no further branching points). Consider an oriented shape $S' \subset S$. An **external neighbour** of S' is a coordinate in S but not in S' that

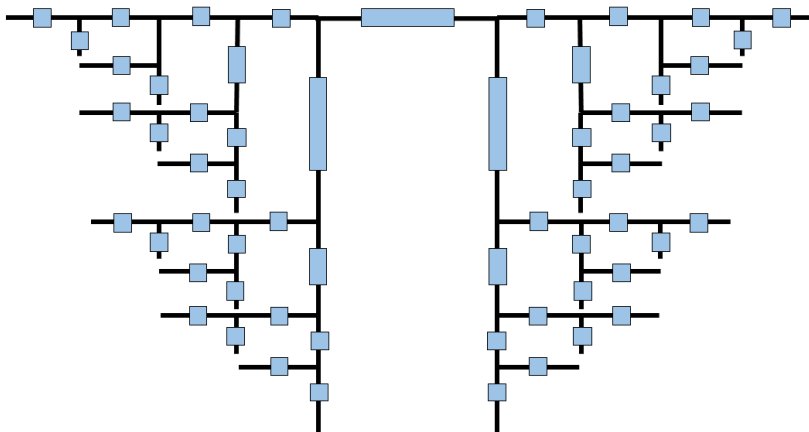


Fig. 12: An abstract schematic of a treeangle of order 2. Black lines represent straight segments of tiles, while blue rectangles represent canvases, each containing distinct self-avoiding walks.

neighbours a coordinate in S' . We may now proceed to our final set of proofs in which we finally prove that the sequenced aTAM requires an unbounded number of tile types to assemble arbitrary treeangles, and thus cannot admit a universal assembly kit.

Lemma 3 Consider a sequenced aTAM instance $\mathcal{P} = (A_{\text{empty}}, Q, g)$ that deterministically assembles a treeangle \bar{S} of order V . Then, the number of unique tile types required in Q grows with at least $\frac{V}{4}$.

Proof For simplicity, consider a specific oriented shape $S \in \bar{S}$ and consider the graph $G_S(S)$. Let R_V , I and \tilde{R}_V be defined as in Definition 6. Then, the subshape defined by any path P from R_V or I to a terminal branching point of \tilde{R}_V , excluding the terminal branching point, must have at least V external neighbours. Consider then a shape S' with P as a subshape, such that S' does not contain any terminal branching points of R_V . Without loss of generality, starting assembly at any coordinate of I or R'_V , any complete trajectory Ψ of \mathcal{P} that assembles S must admit an element A' such that $E(A') = S'$ for some S' (an analogous argument applies for trajectories starting at a coordinate of R_V), since there must exist some time point where the first terminal branching point is incorporated onto S . Furthermore, S' can have no fewer than V external neighbours, because the inclusion of further branching points of R_V can only ever increase the number of external neighbours of S' , and since S' does not contain a terminal branching point of R_V , then the number of external neighbours cannot be decreased by the addition of more coordinates onto S' . By the construction rules of the treeangle, a partition of S as $S = \bigcup_{i=0}^M S_i$ following Theorem 3 (as well as Theorem 6 in the Appendix) is then possible with $S_0 = S'$ and $M \geq V$, and the remaining rules are guaranteed by our treeangle construction. Letting Q' be the subsequence of Q after the assembly time in which A' appears, the sequenced aTAM instance (A', Q', g) requires at least

$\frac{V}{4}$ unique tile types in A' to assemble \bar{S} deterministically. Since all non-empty tile types in A' must appear in Q , Q requires at least $\frac{V}{4}$ unique tile types, completing the proof. \square

Theorem 4 *The sequenced aTAM does not admit a universal assembly kit.*

Proof We only need to show that given any positive integer V , some treeangle \bar{S} of order V exists. The number of walks in any $\mathbb{W}_{L,L,L,L}$ increases monotonically with L . Each $\mathbb{W}_{L,L,L,L}$ is non-empty as a simple straight line fulfilling length constraints will be in this set. Increasing L monotonically increases the number of shapes in $\mathbb{W}_{L,L,L,L}$, as we can simply extend the walk in the canvas with another straight segment or some number of curved walks. Hence, there is always some L that will provide sufficient walks to generate a treeangle \bar{S} of arbitrary order V . This argument extends to other sets $\mathbb{W}_{d,c,c',d'}$. The proof then follows from Lemma 3. \square

3.4 Comparing the Backbone and Sequenced aTAM: The Role of Geometric Constraints

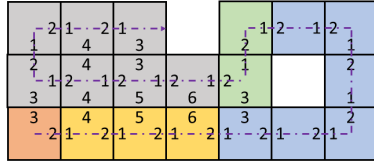
The loss of geometric constraint (that additional tiles must neighbour immediately preceding tiles) when moving from the backbone aTAM to the sequenced aTAM has two effects. Firstly, the shape space of the sequenced aTAM is much larger than the backbone aTAM. The backbone aTAM's shape space is equal to the set of self-avoiding walks, which grows with shape size N as $O(2.638^N)$ from (Clisby and Jensen (2012)). By contrast, the shape space of the sequenced aTAM is equal to the shape space of base temperature-1 aTAM (counting only finite shapes), since a sequence Q can always be constructed by identifying the added tile for any assembly sequence of the temperature-1 base aTAM, assuming the latter is single-tile seeded, allows tile rotations and bans specific mismatches. This space, the set of polyominoes, scales as $O(4.5252^N)$ (Barequet and Shalah (2022)).

We might argue that the loss a universal assembly kit for the sequenced aTAM is simply due to this increase in its shape space. However, even though the shape space of the sequenced aTAM scales faster with N than the shape space of the backbone aTAM, that growth is still exponential. The set of sequences of a given length drawing from a finite k -size alphabet similarly scales exponentially as $O(k^N)$. Hence, combinatorial arguments alone do not preclude the existence of some fixed tile type set with $k \geq 5$ that covers the shape space of the sequenced aTAM.

The second factor at play is that the restriction in tile placement conveys some *advantages* in allowing the backbone aTAM to assemble a complex shape with a small number of tiles. Consider, for example, the configuration shown in Figure 13 (a); the sequence of tiles shown and interaction function in Theorem 2 will deterministically produce the given shape with the backbone aTAM, starting from an empty configuration. By contrast, using the same model inputs (A_{empty}, Q, g) but employing the placement rules of the sequenced aTAM, assembly is not deterministic. The shape in Figure 13 (b) can form if the first blue tile binds to a face on the far side of the growing assembly.

Can the geometric constraint of the backbone aTAM be generalized such that the ability to assemble all shapes in the shape space of the sequenced aTAM? Klarner showed in (Klarner (1967)) that any polyomino can be uniquely defined by labelling

(a)



(b)

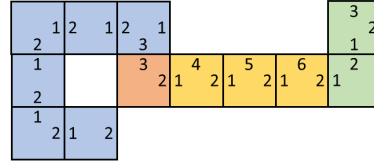


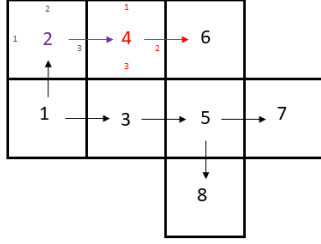
Fig. 13: Geometric constraints due to the backbone can improve determinism. **(a)** The sequence shown (starting with the orange tile) will deterministically produce the shape shown in the backboneed aTAM, given an empty initial configuration and the interaction function in Equation 2. **(b)** The sequenced aTAM, using the same initial configuration, interaction function and sequence can produce both (a) and (b), and hence is not deterministic.

its squares iteratively, starting from neighbours of the squares with the current lowest label (Figure 14.a). It may thus be possible to define a ‘queue-like’ assembly scheme that operates based on this principle, adding future tiles preferentially to existing tiles that were filled earliest in the assembly process (Figure 14.b), although we have not proved this. If so, by returning a sense of geometrical constraint to the sequenced aTAM, a finite universal assembly kit would be recovered (interestingly, this approach requires endowing the assembly scheme with an unbounded memory of the order of added tiles). From this perspective, the loss of a geometrical constraint translates to a loss of shape space-covering power.

If the geometrical restrictions of the backbone appear to provide an advantage, it is natural to ask whether a finite assembly kit exists that allows the sequenced aTAM to deterministically assemble any shape in the shape space of the backboneed aTAM. If we allow for neutral faces, identifying such a kit is trivial, as our construction in Theorem 1 would still satisfy the sequenced aTAM. However, as we have argued, assembly without neutral interactions is conceptually more interesting. Clearly, the construction in Theorem 2 does not work for the sequenced aTAM. When attempting to produce rectangles of m rows and n columns (as in Section 3.2) with the sequenced aTAM $\mathcal{P}_{m,n} = (A_{empty}, Q_{m,n}, g)$ using a sequence $Q_{m,n}$ and interaction function g derived from the constructive proof of Theorem 2, $\mathcal{P}_{m,n}$ fails to deterministically produce the desired rectangle for any $n > 2$ (except when $(m, n) = (2, 3)$). However, we have thus far been unable to prove or disprove the existence of a finite tile type set for the sequenced aTAM that can deterministically assemble any Hamiltonian path shape without relying on neutral interactions. We now present a partial result towards such a proof.

We propose a scheme for assembling any enclosed shape in the sequenced aTAM without relying on neutral interactions. We define an **enclosed shape** as any shape with a well defined Hamiltonian-cycle boundary, that additionally also contains all points within this boundary. Additionally, we also require that the Hamiltonian cycle

(a)



(b)

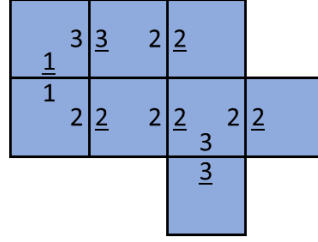


Fig. 14: (a) Illustration of Klarner's rules for enumerating squares in a polyomino. Labelling begins at the lowest square in the leftmost column. The next square is selected by considering neighbours of the lowest labelled square, and going clockwise from the face connecting the existing square to the original polyomino (or from the north facing face for the first square; examples in purple and red provided in the figure). Any polyomino can be uniquely enumerated in this way. (b) A possible labelling scheme under an assembly scheme where tiles are added following a queue, preferentially adding tiles to neighbouring tiles added earlier during assembly. Glue x attracts \underline{x} , and blank faces are assigned a neutral 0 glue.

boundary has no coordinate that neighbours more than two coordinates within the boundary.

Theorem 5 *There exists a finite tile type set with associated interaction function g such that, for any enclosed shape, a sequenced aTAM instance (A_{empty}, Q, g) with elements Q drawn from this tile set that deterministically assembles this shape.*

Proof Let g , with domain $[0, 5] \times [0, 5]$ and $g(\sigma, \sigma') = g(\sigma', \sigma)$, be defined as follows:

$$g(\sigma, \sigma') = \begin{cases} 1, & \text{if } (\sigma, \sigma') = (1, 2), (\sigma, \sigma') = (3, 4), (\sigma, \sigma') = (4, 4) \text{ or } (\sigma, \sigma') = (5, 5) \\ -3, & \text{otherwise.} \end{cases} \quad (3)$$

Then, consider a the subset of the interacting directed tiles from Theorem 2 that only contain 3 as a non-backbone glue type. Any enclosed shape can be constructed by drawing the boundary with interacting directed tiles, with the non-backbone glue 3 facing inwards towards the shape interior. Finally, the interaction between the first and last added boundary tile is encoded by $(5, 5)$. Then, the remainder of the sequence Q is filled with the tile type $\{4, 4, 4, 4\}$ to fill in the shape (Figure 15). \square

We end by noting that, just as tile sequences that deterministically assemble a shape in the backboneed aTAM may fail if used in the corresponding sequenced aTAM instance, sequenced aTAM instances cannot generally be directly converted into a backboneed aTAM instance that deterministically assembles a shape. For instance, using the scheme in Theorem 5 my fail for a backboneed aTAM instance. For a large enough shape, the trajectory may take an arbitrary route inside the interior yellow portion of the shape instead of filling it completely.

with neutral interactions, we have identified a universal assembly kit that almost reaches this limit; the shape space scales as $O(2.638^N)$, implying at least 3 distinct tiles are required, and the universal assembly kit contains only 4 tiles, one of which is only used at the start of a sequence. For the model excluding neutral interactions, the universal assembly kit we have identified is much less efficient, as it contains 208 tiles. With this kit, many sequences must form identical structures, others will be non-deterministic and some will be prematurely terminated. These contributions will be even more dominant for the sequenced aTAM, whose shape space scales as $O(4.5252^N)$ but for which no universal assembly kit exists. The extent to which the different factors contribute to inefficiency in specifying a shape with a sequence are an intriguing unresolved question.

This highly abstract study was initially motivated by the biologically relevant question of what a pre-formed backbone contributes to the self-assembly of RNA and proteins. Our results suggest that, at least in simplified models, the presence of a backbone has a qualitative, rather than merely quantitative, effect on the number of structures that can be reliably formed with a finite set of building blocks, and that both the sequence and the geometric constraints imposed by the backbone are important in directing successful assembly. These results are likely to generalise beyond the specific details of the model considered here, but it would also be instructive to explore more realistic models. In particular, biological assembly occurs at finite temperature with interactions of moderate strength. Contacts can form and break, and cooperativity between units is essential in forming long-lasting bonds. Indeed, the need for cooperative interactions may explain how RNA folding can operate with only 4 unique bases, and protein folding can occur with only 20 different side chains; in practice, cooperatively interacting domains likely provide a much larger effective set of building blocks to direct assembly. Testing this hypothesis with a model of backbone assembly that incorporates finite interaction strengths and cooperative bonding would be a natural next step.

References

- Ahnert, S.E., I.G. Johnston, T.M.A. Fink, J.P.K. Doye, and A.A. Louis. 2010. Self-assembly, modularity, and physical complexity. *Physical Review E* 82(2): 026117. <https://doi.org/10.1103/PhysRevE.82.026117> .
- Anfinsen, C.B. 1972. The formation and stabilization of protein structure. *Biochemical Journal* 128(4): 737–749. <https://doi.org/10.1042/bj1280737> .
- Barequet, G. and M. Shalah. 2022. Improved upper bounds on the growth constants of polyominoes and polycubes. *Algorithmica* 84(12): 3559–3586. <https://doi.org/10.1007/s00453-022-00948-6> .
- Bohlin, J., A.J. Turberfield, A.A. Louis, and P. Šulc. 2023. Designing the self-assembly of arbitrary shapes using minimal complexity building blocks. *ACS Nano* 17(6): 5387–5398. <https://doi.org/10.1021/acsnano.2c09677> .

- Clisby, N. and I. Jensen. 2012. A new transfer-matrix algorithm for exact enumerations: self-avoiding polygons on the square lattice. *Journal of Physics A, Mathematical and Theoretical* 45(11): 115202. <https://doi.org/10.1088/1751-8113/45/11/115202> .
- Demaine, E.D., M.L. Demaine, S.P. Fekete, M.J. Patitz, R.T. Schweller, A. Winslow, and D. Woods. 2012. One tile to rule them all: Simulating any turing machine, tile assembly system, or tiling system with a single puzzle piece. *ArXiv*. <https://doi.org/10.48550/arXiv.1212.4756> .
- Doty, D., J.H. Lutz, M.J. Patitz, S.M. Summers, and D. Woods. 2010. Intrinsic universality in self-assembly. *Proceedings of the 27th International Symposium on Theoretical Aspects of Computer Science: 275–286*. <https://doi.org/10.4230/LIPIcs.STACS.2010.2461> .
- Doty, D., M.J. Patitz, and S.M. Summers. 2011. Limitations of self-assembly at temperature 1. *Theoretical Computer Science* 412(1–2): 145–158. <https://doi.org/10.1016/j.tcs.2010.08.023> .
- Dunn, K.E., F. Dannenberg, T.E. Ouldrige, M. Kwiatkowska, A.J. Turberfield, and J. Bath. 2015. Guiding the folding pathway of DNA origami. *Nature* 525(7567): 82–86. <https://doi.org/10.1038/nature14860> .
- Geary, C., P.É. Meunier, N. Schabanel, and S. Seki. 2019. Oritatami: A computational model for molecular Co-Transcriptional folding. *International Journal of Molecular Science* 20(9). <https://doi.org/10.3390/ijms20092259> .
- Geary, C., P.W. Rothmund, and E.S. Andersen. 2014. A single-stranded architecture for cotranscriptional folding of RNA nanostructures. *Science* 345(6198): 799–804. <https://doi.org/10.1126/science.1253920> .
- Greenbury, S.F., I.G. Johnston, A.A. Louis, and S.E. Ahnert. 2014. A tractable genotype–phenotype map modelling the self-assembly of protein quaternary structure. *Journal of The Royal Society Interface* 11(95): 20140249. <https://doi.org/10.1098/rsif.2014.0249> .
- Han, D., X. Qi, C. Myhrvold, B. Wang, M. Dai, S. Jiang, M. Bates, Y. Liu, B. An, F. Zhang, H. Yan, and P. Yin. 2017. Single-stranded DNA and RNA origami. *Science* 358(6369): eaao2648. <https://doi.org/10.1126/science.aaO2648> .
- Ke, Y., L.L. Ong, W.M. Shih, and P. Yin. 2012. Three-dimensional structures self-assembled from DNA bricks. *Science* 338(6111): 1177–1183. <https://doi.org/10.1126/science.1227268> .
- Klarner, D.A. 1967. Cell growth problems. *Canadian Journal of Mathematics* 19: 851–863. <https://doi.org/10.4153/CJM-1967-080-4> .

- Kočar, V., J.S. Schreck, S. Čeru, H. Gradišar, N. Bašić, T. Pisanski, J.P. Doye, and R. Jerala. 2016. Design principles for rapid folding of knotted DNA nanostructures. *Nature Communications* 7(1): 10803. <https://doi.org/10.1038/ncomms10803> .
- Lau, K.F. and K.A. Dill. 1989. A lattice statistical mechanics model of the conformational and sequence spaces of proteins. *Macromolecules* 22(10): 3986–3997. <https://doi.org/10.1021/ma00200a030> .
- Maňuch, J., L. Stacho, and C. Stoll. 2009. Two lower bounds for self-assemblies at temperature 1. *Proceedings of the 2009 ACM Symposium on Applied Computing*: 808–809. <https://doi.org/10.1145/1529282.1529453> .
- McMullen, A., M. Muñoz Basagoiti, Z. Zeravcic, and J. Brujic. 2022. Self-assembly of emulsion droplets through programmable folding. *Nature* 610(7932): 502–506. <https://doi.org/10.1038/s41586-022-05198-8> .
- Meunier, P.E., D. Regnault, and D. Woods. 2020. The program-size complexity of self-assembled paths. *Proceedings of the 52nd Annual Symposium on Theory of Computing*: 727–737. <https://doi.org/10.1145/3357713.3384263> .
- Meunier, P.E. and D. Woods. 2017. The non-cooperative tile assembly model is not intrinsically universal or capable of bounded turing machine simulation. *Proceedings of the 49th Annual Symposium on Theory of Computing*: 328–341. <https://doi.org/10.1145/3055399.3055446> .
- Mohammed, A.M. and R. Schulman. 2013. Directing self-assembly of DNA nanotubes using programmable seeds. *Nano Letters* 13(9): 4006–4013. <https://doi.org/10.1021/nl400881w> .
- Rothmund, P.W.K. 2006. Folding DNA to create nanoscale shapes and patterns. *Nature* 440(7082): 297–302. <https://doi.org/10.1038/nature04586> .
- Rothmund, P.W.K. and E. Winfree. 2000. The program-size complexity of self-assembled squares. *Conference Proceedings of the Annual ACM Symposium on Theory of Computing*: 459–468. <https://doi.org/10.1145/335305.335358> .
- Russo, J., F. Romano, L. Kroc, F. Sciortino, L. Rovigatti, and P. Šulc. 2022. SAT-assembly: a new approach for designing self-assembling systems. *Journal of Physics: Condensed Matter* 34(35): 354002. <https://doi.org/10.1088/1361-648X/ac5479> .
- Sartori, P. and S. Leibler. 2020. Lessons from equilibrium statistical physics regarding the assembly of protein complexes. *Proceedings of the National Academy of Sciences* 117(1): 114–120. <https://doi.org/10.1073/pnas.1911028117> .
- Seeman, N.C. and H.F. Sleiman. 2017. DNA nanotechnology. *Nature Reviews Materials* 3(1): 17068. <https://doi.org/10.1038/natrevmats.2017.68> .

- Shih, W.M., J.D. Quispe, and G.F. Joyce. 2004. A 1.7-kilobase single-stranded DNA that folds into a nanoscale octahedron. *Nature* 427(6975): 618–621. <https://doi.org/10.1038/nature02307> .
- Soloveichik, D. and E. Winfree. 2007. Complexity of self-assembled shapes. *SIAM Journal on Computing* 36(6): 1544–1569. <https://doi.org/10.1137/S0097539704446712> .
- Videbaek, T., H. Fang, D. Hayakawa, B. Tyukodi, M. Hagan, and W. Rogers. 2022. Tiling a tubule: How increasing complexity improves the yield of self-limited assembly. *Journal of Physics: Condensed Matter* 34(13): 134003. <https://doi.org/10.1088/1361-648X/ac47dd> .
- Woods, D. 2015. Intrinsic universality and the computational power of self-assembly. *Philosophical Transactions of the Royal Society A* 373(2046): 20140214 .
- Young, K.G., B. Najafi, W.M. Sant, S. Contera, A.A. Louis, J.P.K. Doye, A.J. Turberfield, and J. Bath. 2020. Reconfigurable T-junction DNA origami. *Angewandte Chemie International Edition* 59(37): 16076–16080 .
- Zhou, L., D.K. O’Flaherty, and J.W. Szostak. 2020. Assembly of a ribozyme ligase from short oligomers by nonenzymatic ligation. *Journal of the American Chemical Society* 142(37): 15961–15965. <https://doi.org/10.1021/jacs.0c06722> .

Funding. JEG was supported by an Imperial College President’s PhD Scholarship, and TEO by a Royal Society University Research Fellowship.

Acknowledgments. We thank Ard Louis, Jordan Juritz and Benjamin Qureshi for their helpful discussions.

Declarations

All authors certify that they have no affiliations with or involvement in any organization or entity with any financial interest or non-financial interest in the subject matter or materials discussed in this manuscript.

Appendix A Proof that an Unbounded Number of Tile Types are Required for the Sequenced aTAM with Repulsive Interactions

Theorem 6 below replaces Theorem 3 in the main text for the case where repulsive interactions are permitted. Theorem 6 has additional assumptions on the properties of the shape in question relative to Theorem 3, but the treeangle shape defined in the main text was constructed to satisfy this extended set of assumptions. Hence, Theorem 6 leads directly into Lemma 3 in the main text.

Now, we extend the arguments from Theorem 3 for cases where the strength function g is allowed to take on the values $g < 0$. The only difference is we now need to consider tile placement being blocked by repulsion, rather than just overlap of tiles, which could in principle result in the growth of distinct shapes from the same glue type. To understand how this may happen, consider the following set up. Let Ψ be a complete trajectory of \mathcal{P} , with entries $A_t = A_{0,t} + A_{1,t} + A_{2,t} + \dots + A_{M,t}$ where $E(A_i) = S_i$ and $A_{i,t}$ is the subconfiguration of A_i appearing at time t in Ψ . Assuming that two ‘growth’ faces have the same glue $A_0(\ddot{z}_i, \ddot{k}_i) = A_0(\ddot{z}_j, \ddot{k}_j)$, using the approach in Lemma 2, we can construct another ‘partial’ trajectory Ψ' with the subconfigurations $A_{i,t}$ and $A_{j,t}$ swapped that stops at the first time point t_s when repulsion due to an interaction with $g < 0$ precludes a tile from being added to an empty coordinate for the first time. As with Theorem 2, we can write $A'_t = A_0 + A_{i \rightarrow j,t} + A_{j \rightarrow i,t} + A_{c,t}$ as the entries of the trajectory Ψ' . (As a reminder, $A_{j \rightarrow i}$ represents the configuration A_j transformed so that it now ‘grows’ from (\ddot{z}_i, \ddot{k}_i) instead).

For this trajectory Ψ' , at some time t_s , a single tile configuration a_i^{des} with tile consistent with entry t_s of Q forms an attractive interaction with configuration $A_{j \rightarrow i,t_s}$, but is prevented from being added because it forms some repulsive interaction with another tile. We call a_i^{des} a **destabilizing tile**, and its corresponding coordinate z_i^{des} a **destabilizing coordinate**. The trajectory Ψ' can then proceed, and eventually terminate either prematurely or when the last tile of Q is reached, thus Ψ' is a complete trajectory. In this complete trajectory, say $A_{j \rightarrow i,t_s}$ grows into a configuration $A'_{j \rightarrow i}$. As a result of the tile blocking event arising from a_i^{des} , it is possible that deterministic growth can occur that results in $E(A'_{j \rightarrow i}) = E(A_i) \not\approx E(A_j)$ and $E(A'_{i \rightarrow j}) = E(A_j) \not\approx E(A_i)$. Repulsion-derived tile blocking can thus cause the reasoning in Theorem 3 to fail.

The remainder of this appendix is dedicated to illustrating how we can get around this potential failure mode. We begin with a few additional definitions. The **distance** between two points (x_1, y_1) and (x_2, y_2) is taken to be $|x_2 - x_1| + |y_2 - y_1|$. A **subtree subshape** s of an oriented shape S is a subshape of S with a unique **root** in s and its neighbouring **origin** outside of s but in S (Figure 16). The adjacency graph $G_S(s)$ forms a tree and all non-root leaf nodes in $G_S(s)$ are leaf nodes in $G_S(S)$. Additionally, each subtree subshape is uniquely specified by its **root** and **origin**. Now, we proceed to tighten our definition of the target shape to ensure that tile blocking doesn’t invalidate our line of reasoning.

Definition 7 Consider an oriented shape $S = \bigcup_{i=0}^M S_i$. S is a **target shape** with **starting shape** S_0 if it obeys the following assumptions:

1. For any $i, j \in 1, \dots, M$, S_i is not connected to any S_j if $i \neq j$.
2. For any $i \in 1, \dots, M$, S_i has exactly one coordinate that neighbours a coordinate in S_0 , and S_0 has exactly one coordinate that neighbours this coordinate. We denote by \dot{z}_i the coordinate in S_i and by \ddot{z}_i the neighbouring coordinate in S_0 .
3. For any $i \in 1, \dots, M$, $G_S(S_i)$ is a tree with at least one branching node, and with branching points in S_i labelled $v_{i,n}$. Then, every subtree subshape with origin at some $v_{i,n}$ has a unique shape (Figure 16).

4. For any $i \in 1, \dots, M$, $j \in 1, \dots, M$ and $i \neq j$, S_i and S_j have no coordinates within a distance 2 of each other if $\ddot{z}_i \neq \ddot{z}_j$. If $\ddot{z}_i = \ddot{z}_j$, then \dot{z}_i is exactly distance 2 from \dot{z}_j , but no other coordinates in S_i are within distance 2 of any other coordinate in S_j (Figure 17.a).
5. For any $i \in 1, \dots, M$, S_i has no coordinate which is within distance 2 from any coordinate in S_0 , except for \dot{z}_i or its neighbours. There is exactly one coordinate in S_0 at a distance of 2 from \dot{z}_i , which must be some neighbour of \ddot{z}_i . \ddot{z}_i is the only coordinate in S_0 that can be distance 2 from any neighbour of \dot{z}_i within S_i (Figure 17.b).
6. Every straight line segment in S is of at least length 4.
7. S and S_0 have rotational symmetry 1. Additionally, there does not exist S_t , a subshape of S , such that $S_t \neq S_0$ but $S_t \simeq S_0$.

Having expanded our assumptions on our target shape, we wish to consider when repulsion-induced blocking may or may not be significant for our arguments. Consider a sequenced aTAM instance $\mathcal{P} = (A_0, Q, g)$ that produces a target shape S from starting shape that $S_0 = E(A_0)$. The terminal configuration A_w of a trajectory of \mathcal{P} has subconfigurations A_i such that $E(A_i) = S_i$. Assume that partial sub-configurations A_{j,t_s} and $A_{i,t_s} = A_{j \rightarrow i, t_s}$ could be reached during complete trajectories at some time t_s . We say that j and i are **differentially blocked** if, for some single tile configuration a_j , $A_{j,t_s} + a_j$ can be reached during a complete trajectory but $A_{i,t_s} + a_{j \rightarrow i}$ cannot (or vice versa), due to repulsion-induced blocking (Hence $a_i^{des} = a_{j \rightarrow i}$ is the destabilizing tile with coordinate z_i^{des}). In the following lemma, we show that differential blocking is essential to break the arguments in Theorem 3.

Lemma 4 *Consider a sequenced aTAM instance $\mathcal{P} = (A_0, Q, g)$ that oriented-deterministically produces a target shape S (obeying assumptions in Definition 7) from starting shape that $S_0 = E(A_0)$. In the absence of differential blocking between two subconfigurations anchored to the same glue type, the number of unique tile types required in A_0 grows with at least $\frac{M}{4}$.*

Proof Consider whether it is possible to deterministically produce an assembly with $S_i \not\simeq S_j$ if S_i and S_j are anchored to the same glue type. First, if the addition of a tile to partial subconfigurations corresponding to i and j is never blocked due to some repulsive interaction $g < 0$, then Theorem 3 is sufficient to argue that $S_i \simeq S_j$ necessarily, since the assumptions of Definition 7 are a subset of those of Theorem 6 and the contradictions that arise in Theorem 6 remain upheld.

We now allow for non-differential repulsion-induced tile blocking. Consider (without loss of generality) a non-differential repulsion-induced tile block that occurs when trying to add a tile to a partial configuration A_{i,t_s} , where partial subconfiguration $A_{j,t_s} = A_{i \rightarrow j, t_s}$ can also be reached in a complete trajectory. This non-differential tile block does not result in partial subconfigurations A_{j,t'_s} whose equivalents $A_{i,t'_s} = A_{j \rightarrow i, t'_s}$ cannot be reached in a complete trajectory. Unless differential tile blocking occurs elsewhere, the assumed properties of the target shape then imply that for all partial subconfigurations of A_j that can be reached in a complete trajectory, the equivalent partial subconfiguration of A_i can also be reached and the proof of Theorem 6 still applies. Either $S_i \simeq S_j$ and a violation of assumption 3 of our target shape arises, or growth must be non-deterministic.

Hence, in the absence of differential blocking, each S_i must be anchored to a unique glue type, so at least M glue types are required in A_0 . Since each tile type can contain at most 4 unique glue types, at least $\frac{M}{4}$ tile types, are needed in A_0 to assemble S deterministically. \square

Lemma 4 has the following corollary, which states that we would still need $M/4$ tile types if tile blocking only occurs within given subshapes S_i rather than in between them.

Corollary 2 *Consider a sequenced aTAM instance $\mathcal{P} = (A_0, Q, g)$ that oriented-deterministically produces a target shape S (obeying assumptions in Definition 7) from starting shape that $S_0 = E(A_0)$. If the only tile blocking events are such that each destabilizing coordinate z_i^{des} only neighbours one S_i , the number of unique tile types required in A_0 grows with at least $\frac{M}{4}$.*

Proof We once again assume that S_i and S_j are anchored to the same glue type. Consider (without loss of generality) a tile blocking event in which z_i^{des} only neighbours S_i , and that the tile is being added to the partial subconfiguration A_{i,t_s} . Unless a previous differential blocking event has occurred, from the properties of the target shape, the equivalent partial subconfiguration $A_{j,t_s} = A_{i \rightarrow j, t_s}$ can also be reached in a complete trajectory if assembly is to be oriented-deterministic. $z_{i \rightarrow j}^{des}$ would therefore also experience repulsion-induced blocking, and hence blocking events in which the destabilizing coordinate z_i^{des} only neighbours one S_i are non-differential. This Corollary then follows directly as a result of Lemma 4. \square

Lemma 5 *Consider a sequenced aTAM instance $\mathcal{P} = (A_0, Q, g)$ that oriented-deterministically produces a target shape S (obeying assumptions in Definition 7) from starting shape that $S_0 = E(A_0)$. A differential blocking event with destabilizing coordinate z_i^{des} that neighbours S_i and S_k with $i \neq k$ cannot occur.*

Proof We proceed by assuming that there is such a differential blocking event. Then, we show that one of the assumptions on S laid out in Definition 7 necessarily is necessarily violated as a result of this differential blocking event.

First, assume such a tile blocking event occurs, but z_i^{des} is subsequently filled in at some later time (in the trajectory Ψ'). Then S_i would neighbour S_k , and hence a contradiction arises with either assumption 1 or assumption 2. Hence, we only need to consider differential tile blocks where here z_i^{des} is adjacent to S_i as well as some S_k with $i \neq k$, and z_i^{des} remains unoccupied in A'_ω , the terminal configuration of Ψ' .

We now proceed to argue that in this final case, features of A'_ω result in a final shape S that necessarily breaks one of the assumptions 2-6 of Definition 7. a_i^{des} neighbours some tile $a_{j \rightarrow i}^{att}$ in $A_{j \rightarrow i, t_s}$, onto which it may be attracted, and some other tile a^{rpl} that blocks its addition. Hence, $a_{j \rightarrow i}^{att}$ and a^{rpl} must be of distance 2 from each other. The assumptions on S that we have laid out forbid points belonging to any two distinct S_i and S_j from being within distance 2 of each other, with exceptions around the vicinity of junctions where S_0 meets some S_i . More specifically, in order to fulfill assumptions 4 and 5, $a_{j \rightarrow i}^{att}$ can only occupy the position \dot{z}_i or some neighbour of \dot{z}_i .

Next we show that by occupying one of these positions, one or more of the assumptions regarding S must be broken. We define some coordinate z_i^{nb} that forms a straight line with \dot{z}_i and \ddot{z}_i and neighbours \dot{z}_i . Consider now the following cases, which exhaust the possibilities of differential blocking. We will assume, without loss of generality, that any differential blocking occurs due to a tile being blocked from addition to the subshape S_i .

1. Assume $z_j^{nb} \in S_j$. By assumption 5 and lattice placement rules (as illustrated in Figure 18.a), there is no way for z_i^{nb} to neighbour some other S_k with $k \neq i$, and hence $z_i^{nb} \neq z_i^{des}$. Hence, there is no way to block an incoming tile from occupying z_i^{nb} , and given S_i and S_j are anchored onto the same starting glue types, $z_i^{nb} \in S_i$ if growth is deterministic. Consider then $s_{i,nb}$, the subtree subshape of S_i rooted at z_i^{nb} with origin at \dot{z}_i . $s_{i,nb}$ cannot include neighbours of \dot{z}_i other than the root, otherwise S_i as a whole would not be a tree. Hence, all positions in $s_{i,nb}$ other than z_i^{nb} are at a distance greater than 2 from any other S_k for $k \neq i$ (noting that in assumptions 4 and 5, exceptions only cover \dot{z}_i and its neighbours, so neighbours of z_i^{nb} , their neighbours, and so on cannot invoke either exception). So, no position in $s_{i,nb}$ can neighbour any z_i^{des} that neighbours some $S_k \neq S_i$ (incoming tiles onto positions in and adjacent to $s_{i,nb}$ cannot be blocked except by tiles in $s_{i,nb}$). Hence $s_{i,nb} \simeq s_{j,nb}$ if growth is deterministic. Then, if \dot{z}_i and \dot{z}_j are branching points, assumption 3 is violated. Otherwise, as assumption 3 also requires that each S_i contains a branching point, $s_{i,nb}$ and $s_{j,nb}$ also contain branching points, and so some rooted subtree $s'_{i,nb} \subseteq s_{i,nb} \subseteq S_i$ and $s'_{j,nb} \subseteq s_{j,nb} \subseteq S_j$ are such that $s'_{i,nb} \simeq s'_{j,nb}$, also violating assumption 3.
2. Assume $z_j^{nb} \notin S_j$. For the reasons above, z_j^{nb} cannot be the position of a blocked tile, so $z_i^{nb} \notin S_i$. If \ddot{z}_i is a branching point, the segment $\{\ddot{z}_i, \dot{z}_i\}$ must bend onto a third coordinate that is not z_i^{nb} , resulting in $\{\ddot{z}_i, \dot{z}_i\}$ being a straight line segment of length 2 (Figure 18.b), contradicting assumption 6. If \ddot{z}_i is not a branching point, then by assumption 4, z_i^{des} must neighbour S_0 (since it cannot neighbour any other S_k for $k \neq i$). z_i^{des} also neighbours either \dot{z}_i or one of its neighbours. Assume first it neighbours \dot{z}_i . The position that neighbours z_i^{des} in S_0 must be within distance 2 of \dot{z}_i , so this position necessarily bends onto the segment $\{\ddot{z}_i, \dot{z}_i\}$. This segment, in turn, bends onto a third coordinate that is not z_i^{nb} , and hence $\{\ddot{z}_i, \dot{z}_i\}$ is once again a straight line segment of length 2 (Figure 18.b), contradicting assumption 6. Finally, if z_i^{des} neighbours a neighbour of \dot{z}_i , it must neighbour \ddot{z}_i as well by assumption 5. Similarly, the equivalent position $z_{i \rightarrow j}^{des}$ must neighbour S_0 . Thus either blocking is non-differential, or the structure violates assumption 2.

Hence, a contradiction in one of our assumptions arises if a differential block with z_i^{des} that neighbours S_i and S_k with $k \neq i$ occurs. \square

Theorem 6 Consider a sequenced aTAM instance $\mathcal{P} = (A_0, Q, g)$ that deterministically produces a target shape S (obeying assumptions in Definition 7) from a starting shape $S_0 = E(A_0)$. The number of unique tile types required in A_0 grows with at least $\frac{M}{4}$.

Proof Assumption 7 and determinism imply that \mathcal{P} is oriented-deterministic. As per Lemma 4 and Corollary 2, only differential blocking where z_i^{des} neighbours S_i and S_k with $k \neq i$ will allow A_0 to require fewer than $\frac{M}{4}$ tile types. However, Lemma 5 shows that such a differential tile block necessarily results in S failing one of assumptions 2- 6 in Definition 7. Hence, a target shape fulfilling the assumptions of Definition 7 cannot be deterministically assembled by \mathcal{P} if A_0 has fewer than $\frac{M}{4}$ tile types. \square

The treeangle shape defined in the main text was constructed such that it can be partitioned in a way that satisfies the assumptions of Definition 7. Hence this Theorem

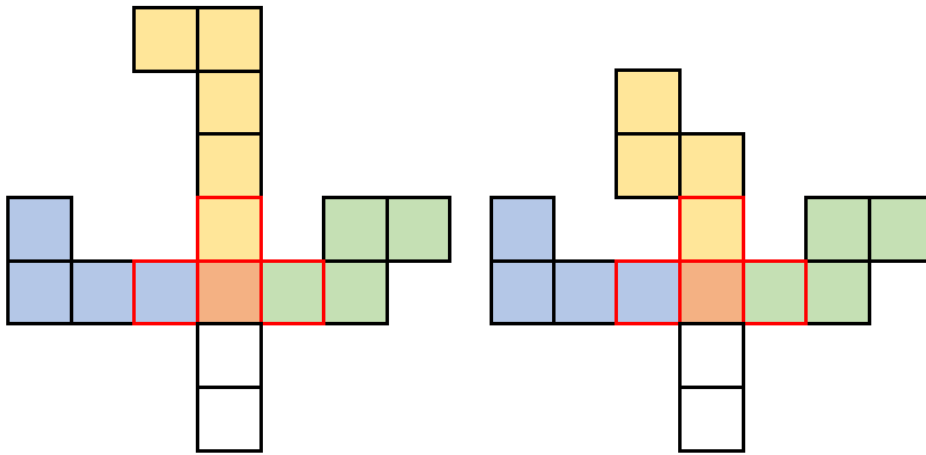
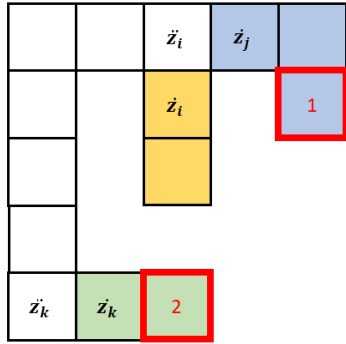


Fig. 16: An illustration of assumption 3 in the definition of shapes S_i used in Theorem 6. The two shapes are two instances of S_i , where the lower white tiles connect to some larger S_0 . A single branching point (also the **origin tile** of the subtree subshapes) is given in orange, while **root tiles** are outlined in red. The left oriented shape obeys assumption 3, as each subtree subshape (coloured in blue, yellow and green) are distinct, while the right oriented shape violates this assumption as the yellow rooted subtree subshape is equivalent to the green under a 90° clockwise rotation followed by a $(1, -1)$ translation.

can be used in the proof of Lemma 3, taking the place of Theorem 3 which is only valid if $g \geq 0$.

(a)



(b)

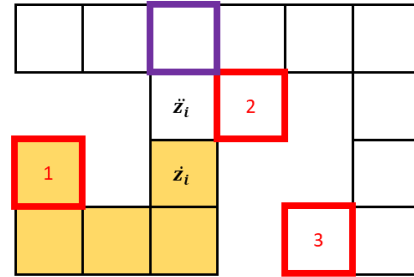


Fig. 17: Illustrations of assumptions 4 and 5 in the definition of shapes in Theorem 6. Tiles belonging to S_0 are in white, and tiles belonging to each S_i are assigned a single color. Tiles violating assumptions are outlined in red. **a.** An illustration of how assumption 4 can be violated. Violation 1 is due to a tile of S_j (with $\ddot{z}_j = \ddot{z}_i$) that is not \dot{z}_j being within distance 2 of \dot{z}_i , while violation 2 is due to a tile of S_k ($\ddot{z}_k \neq \ddot{z}_i$) being within distance 2 of an arbitrary tile of S_i . **b.** An illustration of how assumption 5 can be violated. Violation 1 is due to a tile of S_0 being within distance 2 of a tile of S_i , with both tiles being far from \ddot{z}_i and \dot{z}_i . Violation 2 is due to two tiles (the violating tile and the purple outlined tile) in S_0 being within distance 2 of \dot{z}_i . Finally, violation 3 is due to a tile of S_0 , far from \ddot{z}_i , being within distance 2 of a neighbour of \dot{z}_i .

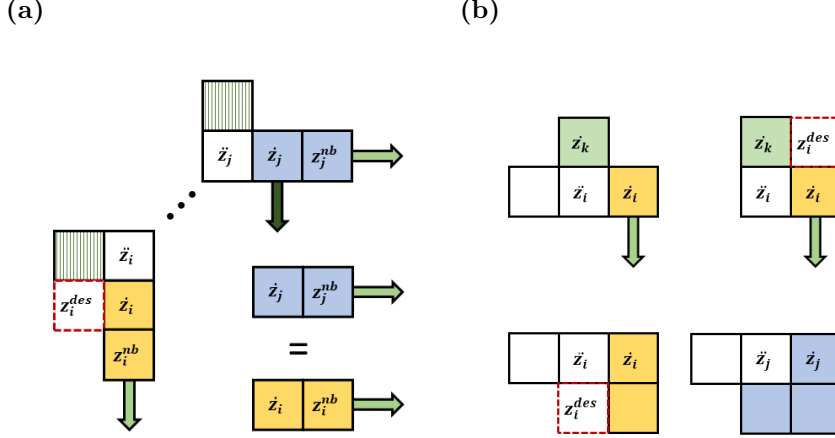


Fig. 18: Theorem 6 lays out two possibilities in the case where a tile-blocked coordinate z_i^{des} remains unfilled at the end of a complete trajectory. We show here fragments of the terminal configuration $A'_{\omega,c}$. $\mathbf{A}_{j \rightarrow i}$ is given in yellow, \mathbf{A}_j is given in blue and **destabilizing tiles** z_i^{des} are in dotted red. We illustrate how the two possibilities violate assumptions on S laid out at the beginning of Theorem 6. **a.** An illustration of how case 1 violates assumptions on S . The striped tile can be either a **tile of \mathbf{A}_0 or z_k** . **Arrows** represent some arbitrary tree-shaped configurations, where arrows of the same color represent configurations with equivalent (up to rotations and translations) shapes. The tile at z_j^{nb} cannot be destabilized upon transformation into z_i^{nb} as it is too far away from any coordinate of S_0 or any other S_k , and hence $z_i^{nb} \neq z_i^{des}$. Since branches that grow from z_i^{nb} are too far away from any S_k for $k \neq i$ to be blocked, The branches that grow from z_i^{nb} and z_j^{nb} must have identical shapes, violating assumptions on the shape S . **b.** An illustration of how case 2 violates assumptions on S . Green tiles are z_k for some $k \neq i, j$. The green arrows represent **arbitrary tree-shaped configurations**. If z_i is branching (Top left), or if z_i^{des} neighbours z_i (Top right), $\{z_i, z_i\}$ is a straight line segment of length 2, breaking assumption 6. Otherwise, if the destabilizing tile neighbours z_i and a neighbour of z_i (Bottom left), but its equivalent is present in S_j , then S_j has two coordinates neighbouring S_0 (Bottom right).